J Math Chem (2011) 49:1115–1127
DOI 10.1007/s10910-011-9809-4

REVIEW

# Orientation of a benzene molecule inside a carbon nanotube

**Thien Tran-Duc · Ngamta Thamwattana · James M. Hill**

Received: 12 July 2010 / Accepted: 17 March 2011 / Published online: 1 April 2011


**Abstract** Benzene molecules confined in carbon nanotubes of varying radii are employed as semiconductors in electronic nanodevices, and their orientation determines the electrical properties of the system. In this paper, we investigate the interaction energy of all the possible configurations of a benzene molecule inside various carbon nanotubes and then we determine the equilibrium configuration. We adopt the continuous approach together with the semi-empirical Lennard-Jones potential function to model van der Waals interaction between a benzene molecule and a carbon nanotube. This approach results in an analytical expression, which accurately approximates the interaction energy and can be readily used to generate numerical data. We find that horizontal, tilted and perpendicular configurations on the axis of the carbon nanotube are all possible equilibrium configurations of the benzene molecule when the radius of the carbon nanotube is less than 5.580 Å. However, when the radius of the carbon nanotube is larger than 5.580 Å an offset horizontal orientation is the only possible equilibrium configuration of the benzene molecule. In the limiting case, the orientation of a benzene molecule on a graphene sheet can be derived simply by letting the radius of the carbon nanotube tend to infinity.

## 1 Introduction

Nowadays, carbon nanotubes have been widely used in many applications of materials science, medicine and biotechnology [1–4], because of their excellent thermal,

T. Tran-Duc (✉) · N. Thamwattana
Nanomechanics Group, School of Mathematics and Applied Statistics, University of Wollongong, Wollongong, NSW 2522, Australia
e-mail: ttd689@uow.edu.au

J. M. Hill
Nanomechanics Group, School of Mathematical Sciences, University of Adelaide, Adelaide, SA 5005, Australia

mechanical, electrical, biological and chemical properties [5,6]. A single-walled carbon nanotube is formed by rolling up a two-dimensional graphene sheet along the chiral vector and therefore they inherit excellent electrical properties of the graphene sheet which is known as a $\pi$-system. Electrical architectures of carbon nanotubes are ideal for applications in semiconductors [7]. Zhou et al. [7] carry out electrical measurements for carbon nanotubes of 2.8 nm and 1.3 nm in diameter at different temperatures. They establish that at room temperature and zero gate voltage, the resistance of the carbon nanotube is in the range of 160–500 k$\Omega$ if the tube diameter is greater than 2.0 nm and of the order of megaohms or higher if the tube diameter is less than 1.5 nm. In other words, the electron transport capacity of carbon nanotubes is directly proportional to their size. Kane and Mele et al. [8] use a theory of long-wavelength low-energy electronic structure to explain the dependence of electronic properties of straight single-walled carbon nanotubes as well as locally twisted and bent carbon nanotubes. Coulomb interactions in carbon nanotubes are also investigated by Kane et al. [9].

The notion of introducing molecules into carbon nanotubes to change their electrical properties for the purpose of creating semiconductors or superconductors to be used in electronic nanodevices has been intensively investigated in recent decades. A novel application formed by inserting $C_{60}$ fullerene molecules into carbon nanotubes are referred to as nanopeapods. The incorporation of fullerenes into carbon nanotubes, which are all $\pi$-systems, creates superconductors because electrons can travel along both the wall of the carbon nanotube and along the fullerenes. The impact of position and orientation of the fullerenes inside carbon nanotubes on the electrical properties of nanopeapods have been studied [2,10]. In a related application, Schulte et al. [11] investigate the encapsulation of phthalocyanine molecules, which are metallo-organic molecules and carry localized magnetic moments, inside carbon nanotubes. Phthalocyanine molecules possess strong optical absorption properties and therefore they have been used in photovoltaic devices [12]. In addition, they also possess very good bulk optical properties, such as dichroism and luminescence, which can be used in gas detection applications [13]. The orientation of the phthalocyanine molecules inside the carbon nanotube affects their optical, magnetic and electrical transport properties, which are investigated experimentally by Schulte et al. [11]. Aromatic hydrocarbon molecules are other molecules which have also received much attention due to their excellent electrical properties. Aromatic hydrocarbon molecules are considered as combinations of one or many rings whose structures are similar to the structure of a benzene molecule. Aromatic hydrocarbon molecules are also $\pi$-systems and therefore they have electrical properties similar to graphene sheets, carbon nanotubes and fullerenes. Electronic confinement effects in carbon nanotubes of some aromatic hydrocarbons, such as benzene, naphthalene and anthracene, have been studied [14]. Among aromatic hydrocarbons, benzene molecules, which have been used in molecular nanodevices [15,16], are normally chosen for study because they possess intrinsic properties of aromatic hydrocarbons and moreover the small size of benzene molecules permits them to be encapsulated easily inside carbon nanotubes of various diameters.

As mentioned above, the orientation and the position of benzene molecules inside carbon nanotubes determines the electrical properties of the whole system. Van der Waals interactions are recognized as the dominant interactions between benzene mol-

ecules as well as between benzene molecules and carbon nanotubes and therefore they are the key factors for determining the particular arrangements of benzene molecules inside carbon nanotubes. The interaction between two benzene molecules, or a benzene dimer, have been studied by many authors [17,18]. These problems are typical for a class of problems of aromatic interactions which are key factors in explaining stabilities of double helices of DNA and the global structure of proteins [19]. A study on the general geometry of a benzene dimer is carried out by the current authors in [20]. In [20], in order to model the interaction in a benzene dimer the present authors use the semi-empirical Lennard-Jones potential function together with a continuous approach, and each benzene molecule is assumed to be a combination of two concentric rings, namely an inner carbon ring and an outer hydrogen ring. The major results in [20] are the determination of an analytical expression for the interaction energy, which readily permits numerical evaluation by algebraic packages, such as Maple or Matlab, and the determination of all possible orientations of a benzene molecule with respect to the other one, as the distance between the two benzene molecules varies. This approach shows that it is much simpler and less computationally intensive than conventional methods, such as *ab*-initio calculations or density functional theory, and moreover it produces a very good approximation to the interaction energy [21]. Moreover, this approach can be readily applied to large molecules, such as carbon nanotubes or graphene sheets. Here, we continue this approach to investigate the interactions of a benzene molecule inside a carbon nanotube and to investigate the arrangements of benzene molecules confined inside carbon nanotubes.

## 2 Mathematical modelling

A benzene molecule comprises six carbon atoms and six hydrogen atoms and the distances from the center of mass to each carbon atom and hydrogen atom are 1.4 and 2.84 Å, respectively. Due to the symmetry of the structure, a benzene molecule can be modelled as two concentric circular rings, an inner ring of carbon atoms and an outer ring of hydrogen atoms (Fig. 1) and the interaction between a benzene molecule and a carbon nanotube may be viewed as the sum of two interactions of rings with the carbon nanotube. The total interaction energy between a benzene molecule and a carbon nanotube is given by

$$E = E_1 + E_2, \tag{1}$$

where $E_1$ and $E_2$ are respectively the interaction energies between the carbon and hydrogen rings and the carbon nanotube.

The mathematical model for the problem of the interaction between a ring and a carbon nanotube is illustrated in Fig. 2. The relative position of the ring with respect to the carbon nanotube is defined by the rotational angle $\phi$ of the plane of the ring about the $y$-axis, an offset distance $\epsilon$ from the center of the ring to the $z$-axis and a rotational angle $\psi$ of the center of the ring about the $z$-axis. The interaction energy between the ring and a carbon nanotube is calculated using the semi-empirical Lennard-Jones potential function as follows,

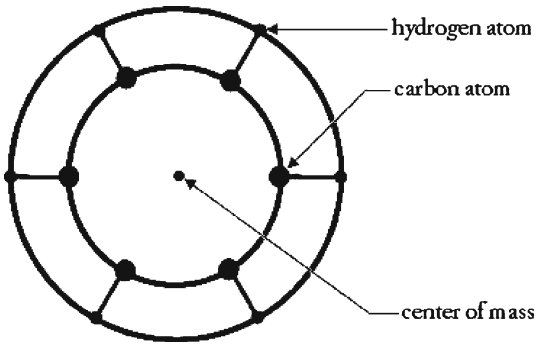


**Fig. 1** Model of benzene molecule with inner carbon ring and outer hydrogen ring

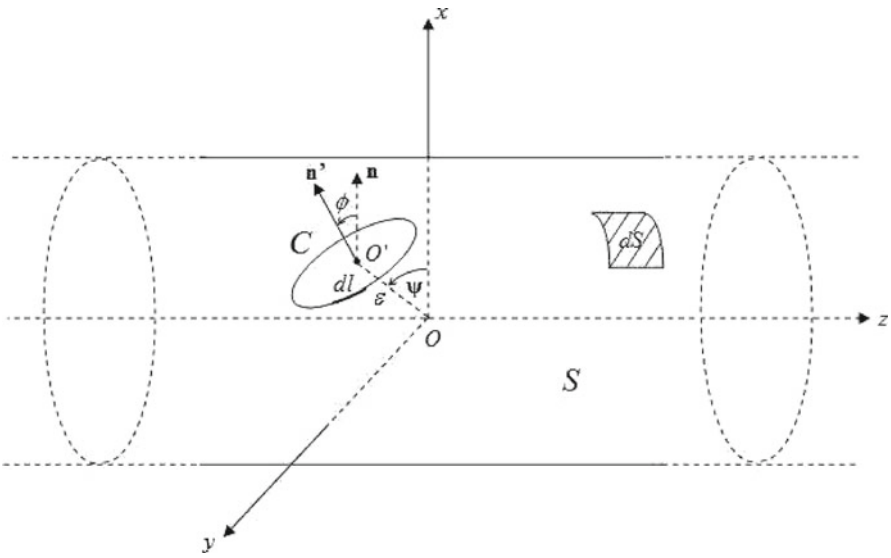


**Fig. 2** Model for interaction between a ring and a tube

$$E_r = \eta_1 \eta_2 \int_C \int_S \left( -\frac{A}{\rho^6} + \frac{B}{\rho^{12}} \right) dS d\ell, \tag{2}$$

where $\rho$ is the Euclidean distance between the line element $d\ell$ on the ring and the surface element $dS$ on the tube, $\eta_1$ and $\eta_2$ are the respectively line and surface atomic densities of the ring and the carbon nanotube, and $A$ and $B$ are the attractive and repulsive constants, respectively. Values of constants used in this paper are shown in Table 1.

For convenience, we may rewrite Eq. (2) as follows;

$$E_r = \eta_1 \eta_2 \left( -A J_3 + B J_6 \right), \tag{3}$$

where

$$J_n = \int_C \int_S \frac{1}{\rho^{2n}} dS d\ell, \tag{4}$$

and the final analytical form of $J_n$ is given by Eq. (A-9).

## 3 Results and discussion

Numerical values of the interaction energy for certain cases of the benzene-carbon nanotube complex which are obtained using the hybrid discrete-continuous approach and the present approach (continuous approach) are shown in Table 2. In the discrete-continuous approach, the interaction energy between the benzene molecule and the carbon nanotube is the sum of twelve interaction energies for six interactions of the carbon atoms with the carbon nanotube and six interactions of the hydrogen atoms with the carbon nanotube. Unlike the continuous approach, one more rotational angle $\theta$ needs to be taken into account to describe the position of each atom on the benzene molecule. Due to the symmetry of the benzene molecule, we only need consider $\theta \in [0, \pi/3)$. From Table 2, we can see that the numerical values for the interaction energies obtained using the continuous approach agree well with those of the discrete-continuous approach.

The equilibrium configuration of the benzene molecule inside a carbon nanotube is the configuration which produces the smallest interaction energy. In general, an equilibrium configuration is determined by a set of values $\epsilon$, $\omega$ and $\phi$ which are the roots of the three-equation system $\partial E/\partial\epsilon = 0$, $\partial E/\partial\omega = 0$ and $\partial E/\partial\phi = 0$. Interestingly, for any given offset distance, the minimum interaction energy is always obtained at $\omega = 0$. As illustrated in Fig. 3, the minimum points on the curves of the interaction energy from $\omega = 0$ are always the lowest interaction energy points regardless

**Table 1** Numerical values of constants used in the model

| | |
|---|---|
| Carbon ring radius | 1.400 (Å) |
| Hydrogen ring radius | 2.480 (Å) |
| CNT (8,6) radius | 4.762 (Å) |
| CNT (9,6) radius | 5.119 (Å) |
| CNT (10,10) radius | 6.780 (Å) |
| CNT (13,13) radius | 8.814 (Å) |
| Carbon ring atomic line density | 0.682 $\left(\text{Å}^{-1}\right)$ |
| Hydrogen ring atomic line density | 0.385 $\left(\text{Å}^{-1}\right)$ |
| CNT atomic surface density | 0.382 $\left(\text{Å}^{-2}\right)$ |
| C-C attractive constant | 560.44 $\left(\text{kcal/mol} \times \text{Å}^6\right)$ |
| C-H attractive constant | 129.67 $\left(\text{kcal/mol} \times \text{Å}^6\right)$ |
| C-C repulsive constant | 1,121,755.66 $\left(\text{kcal/mol} \times \text{Å}^{12}\right)$ |
| C-H repulsive constant | 91,727.95 $\left(\text{kcal/mol} \times \text{Å}^{12}\right)$ |

**Table 2** Interaction energies computed using discrete-continuous and continuous approaches

| $\psi$(rad) | $\phi$(rad) | $\epsilon$(Å) | $R$(Å) | $E_{dis}$ (kcal/mol) | | | $E_{cont}$ (kcal/mol) |
|---|---|---|---|---|---|---|---|
| | | | | $\theta = 0$ | $\theta = \pi/6$ | $\theta = \pi/4$ | |
| 0 | $\pi/2$ | 0 | 5.089 | −17.799 | −17.799 | −17.799 | −17.762 |
| $\pi/8$ | $\pi/3$ | 0.5 | 5.424 | −18.016 | −18.047 | −18.008 | −17.994 |
| $\pi/6$ | $\pi/4$ | 0.85 | 6.102 | −12.755 | −12.758 | −12.738 | −12.730 |
| $\pi/4$ | $\pi/6$ | 0.33 | 5.766 | −14.003 | −13.929 | −13.957 | −13.937 |
| $\pi/3$ | 0 | 1.26 | 6.780 | −8.468 | −8.415 | −8.442 | −8.424 |
| $\pi/2$ | $\pi/5$ | 2.52 | 8.814 | −4.199 | −4.198 | −4.199 | −4.190 |

of the value of $\epsilon$. In other words, the equilibrium configuration is always obtained at $\omega = 0$. Thus, for a given carbon nanotube, we can determine the equilibrium configuration of the benzene molecule by solving the two-equation system, $\partial E/\partial\epsilon = 0$ and $\partial E/\partial\phi = 0$, at $\omega = 0$. However, before determining the equilibrium configuration of the benzene molecule inside a carbon nanotube, we investigate changes occurring in the orientation of the benzene molecule as the offset distance $\epsilon$ varies. The investigation provides an insight into behaviors of the benzene molecule inside a carbon nanotube.

Figure 4 shows the orientations of the benzene molecule which produce the minimum interaction energies as $\epsilon$ changes from zero for the carbon nanotubes (8, 6), (9, 6) and (9, 7). These equilibrium configurations occur on the axis of carbon nanotubes but at different orientations. In more detail, these equilibrium configurations are obtained at $\phi = 0\,(E = -16.159$ kcal/mol), $\phi = 0.913\,(E = -20.414$ kcal/mol) and $\phi = \pi/2\,(E = -19.094$ kcal/mol), respectively, and we refer to them as the horizontal configuration, the tilted configuration and the perpendicular configuration, respectively. Our calculations show that an equilibrium configuration always occurs on the axis for carbon nanotubes provided that $R < 5.580$ Å. The changes that occur in the orientation and the interaction energy for the equilibrium configurations of the benzene molecule when $R$ is less than 5.580 Å are shown in Fig. 5. We see that the horizontal configuration is dominant in the region $R < 4.767$ Å, while the tilted configuration is dominant for values of $R$ in the region of $(4.767,\ 5.425)$ and the perpendicular configuration is the more stable configuration when $5.425\ \text{Å} \leq R \leq 5.580\ \text{Å}$. Among these equilibrium configurations, the equilibrium configuration of the benzene molecule inside a carbon nanotube with $R = 5.115$ Å produces the smallest interaction energy, which occurs at $\phi \approx 52°$ (Fig. 5b). Table 3 shows the results for the equilibrium configurations and the corresponding interaction energies of the benzene molecule inside carbon nanotubes which have radii less than 5.580 Å.

When $R \geqslant 5.580$ Å, the equilibrium configurations no longer occur on the axis of the carbon nanotube but at an offset horizontal configuration. This is the only equilibrium configuration of the benzene molecule inside the carbon nanotubes for which $R \geqslant 5.580$ Å. As illustrated in Fig. 6 which shows orientations of the benzene molecule which produce the minimum interaction energies as $\epsilon$ changes from zero for the carbon nanotubes (10, 10) and (13, 13), respectively, we see that in both cases, the

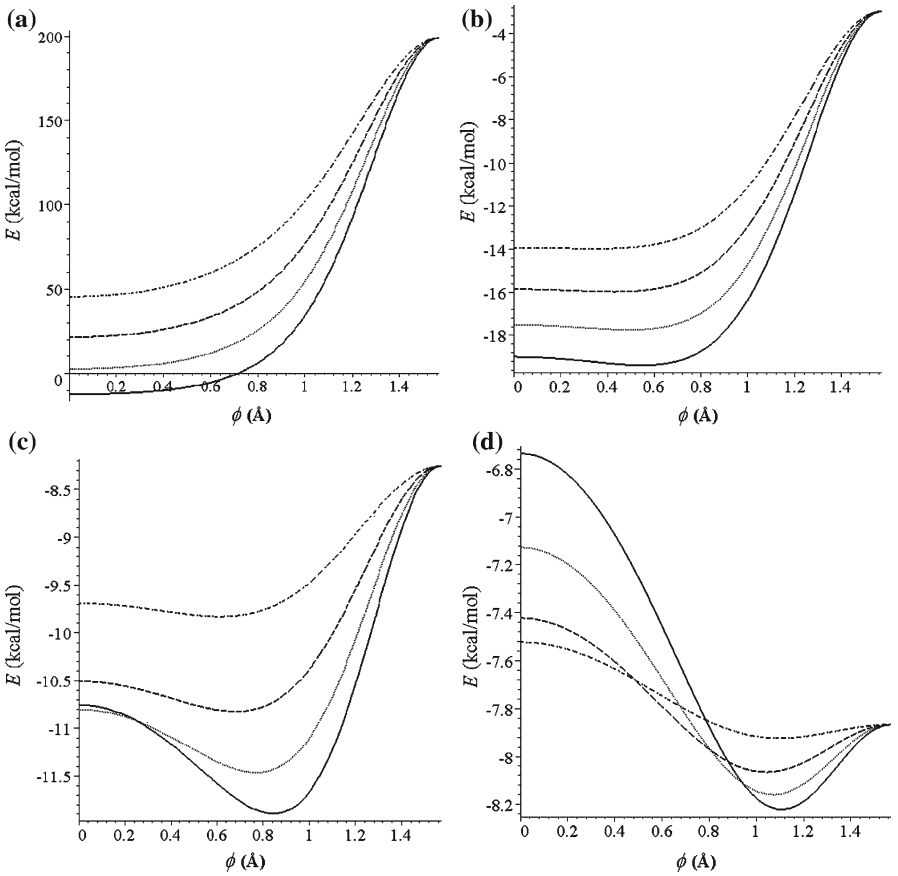


**Fig. 3** Interaction energy distribution: **a** $(\epsilon, R) = (0.6, 4.762)$, **b** $(\epsilon, R) = (0.5, 5.119)$, **c** $(\epsilon, R) = (2.0, 6.780)$, **d** $(\epsilon, R) = (3.8, 8.814)$. The *solid*, *dotted*, *dashed* and *dashed-dotted lines* correspond to $\psi = 0$, $\pi/6$, $\pi/4$, and $\pi/3$, respectively

benzene molecule only obtains an equilibrium configuration at $\phi = 0$ and for a non-zero offset distance. The values of the offset distance and corresponding interaction energy of the equilibrium configurations are 3.021 Å and −15.795 kcal/mol, 5.194 Å and −13.843 kcal/mol, respectively. As $R$ increases, the magnitude of the interaction energy for the equilibrium configurations decreases. Table 4 lists the offset distances and the corresponding interaction energy of some of the equilibrium offset horizontal configurations for the benzene molecule when $R \geqslant 5.580$ Å. In this table, we use $\epsilon_0$ for the offset distance of the equilibrium configuration and $d_0 = R - \epsilon_0$ for the distance from the wall of the carbon nanotube to the center of the benzene molecule. Mathematically, as $R$ tends to infinity, the present problem becomes the problem of the interaction of a benzene molecule with a graphene sheet. This is also reflected in Table 4 as $R$ increases when $d_0$ and the interaction energy of the offset horizontal configurations tend to the values of the distance and interaction energy of the equilibrium parallel configuration of a benzene molecule with a graphene sheet which

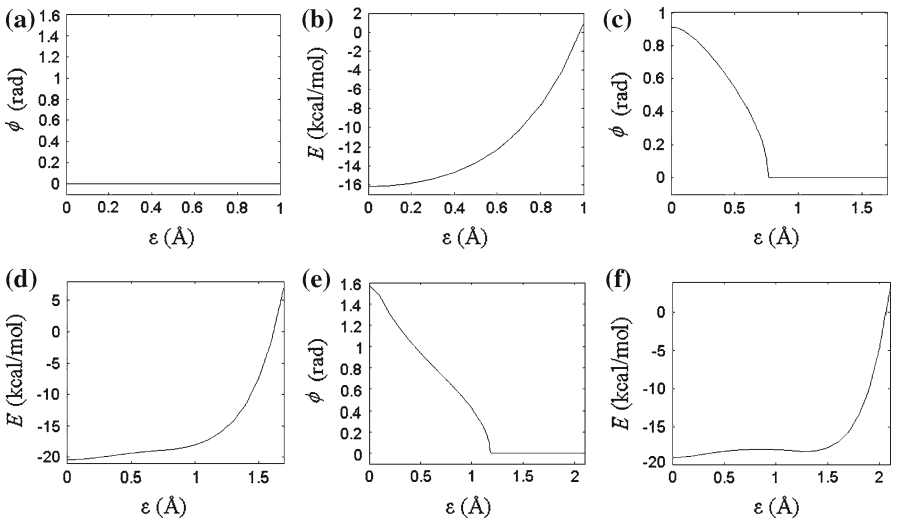


**Fig. 4** Values of interaction energy and rotational angle for configurations producing smallest interaction energies for carbon nanotubes (8, 6) (**a, b**), (9, 6) (**c, d**) and (9, 7) (**e, f**) as the offset distance changes

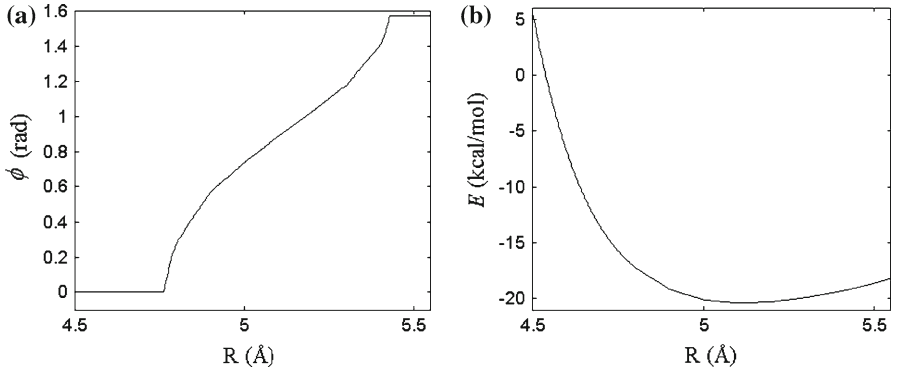


**Fig. 5** Interaction energy distributions at $\epsilon = 0$

are given in [22,23]. Using the van der Waals density functional theory, Chakarova et al. [22] obtain the values of the interaction energy and the equilibrium distance of a benzene molecule with a graphene sheet as $-11.421$ kcal/mol and 3.6 Å, respectively. By measuring the thermal desorption of a benzene molecule on the surface of a graphene sheet, Zacharia et al. [23] also obtain the value of the interaction energy for this configuration to be $-11.5636 \pm 1.846$ kcal/mol.

## 4 Conclusion

In this paper, we model the van der Waals interaction between a benzene molecule and a carbon nanotube by using the continuous approach together with the semi-empirical Lennard-Jones potential function. An analytical expression for the interaction energy

**Table 3** On axis equilibrium configurations inside carbon nanotubes for radii less than 5.580 Å($\phi_0$ is the value of rotational angle)

| Carbon nanotube | $R$ (Å) | $\phi_0$ (rad) | Interaction energy (kcal/mol) | Equilibrium configuration |
|---|---|---|---|---|
| (7,7) | 4.746 | 0 | −15.622 | Horizontal |
| (8,6) | 4.762 | 0 | −16.159 | Horizontal |
| (9,5) | 4.810 | 0.330 | −17.483 | Tilted |
| (8,7) | 5.089 | 0.871 | −20.400 | Tilted |
| (10,5) | 5.178 | 0.995 | −20.344 | Tilted |
| (8,8) | 5.424 | 1.540 | −19.187 | Tilted |
| (9,7) | 5.438 | $\pi/2$ | −19.094 | Perpendicular |
| (10,6) | 5.480 | $\pi/2$ | −18.785 | Perpendicular |

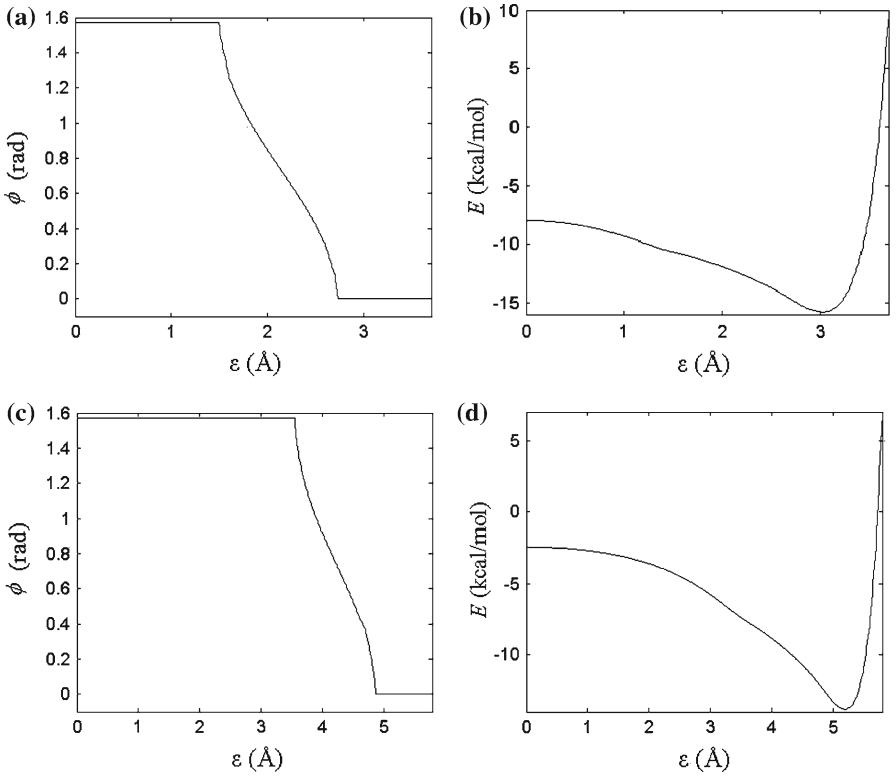


**Fig. 6** Values of interaction energy and rotational angle for configurations producing smallest interaction energies for the carbon nanotubes (10, 10) (**a, b**), (13, 13) (**c, d**) for variable offset distance

is obtained which is used to determine the orientation and position of a benzene molecule inside carbon nanotubes of various radii. We find that there are three different equilibrium configurations of the benzene molecule, namely the horizontal, the tilted and the perpendicular configurations, that become available on the axis of the carbon

**Table 4** Equilibrium offset horizontal configurations for benzene molecule inside carbon nanotubes with $R > 5.580$ Å

| Carbon nanotube | $R$ (Å) | $\epsilon_0$ (Å) | $d_0 = R - \epsilon_0$ (Å) | $E$ (kcal/mol) |
|---|---|---|---|---|
| (11,11) | 7.458 | 3.770 | 3.688 | −14.965 |
| (14,14) | 9.492 | 5.893 | 3.599 | −13.455 |
| (18,15) | 11.202 | 7.450 | 3.752 | −12.817 |
| (20,21) | 13.900 | 10.36 | 3.540 | −12.110 |
| (25,22) | 15.944 | 12.416 | 3.528 | −11.803 |
| (30,28) | 19.666 | 16.156 | 3.510 | −11.465 |
| (35,40) | 25.444 | 21.960 | 3.484 | −11.238 |

$\epsilon_0$ is offset distance from the center of benzene molecule to axis of carbon nanotube, $d_0$ is distance from the wall of carbon nanotube to center of benzene molecule

nanotube as the radius of the tube varies for $R < 5.580$ Å. For $R \geqslant 5.580$ Å, the offset horizontal configuration is the only equilibrium configuration. When the value of $R$ is sufficiently large, the results obtained here become a good approximation for the interaction between a benzene molecule and a graphene sheet. The present study together with [20] for the interaction between two benzene molecules permits the determination of the arrangement of benzene molecules confined inside carbon nanotubes of various radii.

## Appendix A: Analytical evaluation of $J_n$

In this appendix, we provide a formal evaluation of the integrals $J_n$ as defined by Eq. (4) which can be rewritten as

$$J_n = rR \int_0^{2\pi} \int_0^{2\pi} \int_{-\infty}^{\infty} \frac{1}{\rho^{2n}} dz d\beta d\alpha, \tag{A-1}$$

where $\rho^2 = (r\sin\alpha\sin\phi + \epsilon\cos\psi - R\cos\beta)^2 + (r\cos\alpha + \epsilon\sin\psi - R\sin\beta)^2 + (r\sin\alpha\cos\phi - z)^2$ is the distance between a point on the ring and a point on the surface of the carbon nanotube. For convenience, we introduce $K_1 = (r\sin\alpha\sin\phi + \epsilon\cos\psi - R\cos\beta)^2 + (r\cos\alpha + \epsilon\sin\psi - R\sin\beta)^2$ and then we make the substitution $K_1^{1/2}\tan\theta = (z - r\sin\alpha\cos\phi)$ into Eq. (A-1) to obtain

$$J_n = rR \int_0^{2\pi} \int_0^{2\pi} \frac{1}{K_1^{n-\frac{1}{2}}} d\beta d\alpha \int_{-\pi/2}^{\pi/2} \cos^{2n-2}\theta d\theta, \tag{A-2}$$

which can be simplified as follows

$$J_n = \frac{\pi(2n-3)!!rR}{2^{n-1}(n-1)!}\int_0^{2\pi}\int_0^{2\pi}\frac{1}{K_1^{n-\frac{1}{2}}}d\beta d\alpha, \tag{A-3}$$

since $\int_{-\pi/2}^{\pi/2}\cos^{2n-2}\theta d\theta = \pi(2n-3)!!/[2^{n-1}(n-1)!]$. On rewriting $K_1$ as a function of $\beta$, Eq. (A-3) becomes

$$J_n = \frac{\pi(2n-3)!!rR}{2^{n-1}(n-1)!}\int_0^{2\pi}\int_0^{2\pi}\frac{1}{\left[R^2+X^2+2RX\cos(\beta-\beta_0)\right]^{n-\frac{1}{2}}}d\beta d\alpha, \tag{A-4}$$

where $\beta_0 = \arctan((r\cos\alpha + \epsilon\sin\psi)/(r\sin\alpha\sin\phi + \epsilon\cos\psi))$ and $X = [(r\sin\alpha\sin\phi+\epsilon\cos\psi)^2 + (r\cos\alpha+\epsilon\sin\psi)^2]^{1/2}$. The integrand in Eq. (A-4) is a periodic function of $\beta$ with period of $2\pi$, so we may change the limits from $(0, 2\pi)$ to $(\beta_0, 2\pi+\beta_0)$ without changing the value of the integral and therefore we can omit the term $\beta_0$ in Eq. (A-4). On using the trigonometric relationship $\cos\beta = 1-2\sin^2(\beta/2)$ and then substituting $t = \sin^2(\beta/2)$, we obtain the standard integral representation of the hypergeometric function (eqn. (9.311), page 1005, [24]), and Eq. (A-4) can be written as follows

$$J_n = \frac{\pi^2(2n-3)!!rR}{2^{n-2}(n-1)!}\int_0^{2\pi}(R+X)^{1-2n}F\left(n-\frac{1}{2},\frac{1}{2};1;\frac{4RX}{(R+X)^2}\right)d\alpha. \tag{A-5}$$

On using the transformation $(1+z)^{-2a}F\left(a,b;2b;4z/(1+z)^2\right) = F(a,a-b+1/2;b+1/2;z^2)$ (eqn (9.134(3)), page 1009, [24]) for the integrand in Eq. (A-5) with $z = X/R$, we obtain

$$J_n = \frac{\pi^2(2n-3)!!r}{2^{n-2}(n-1)!R^{2n-2}}\int_0^{2\pi}F\left(n-\frac{1}{2},n-\frac{1}{2};1;\frac{X^2}{R^2}\right)d\alpha, \tag{A-6}$$

and since the ring is inside the tube, we have $|X/R| < 1$ and the hypergeometric series is always convergent. Therefore, we can change the orders of the integration and the summation to obtain

$$J_n = \frac{\pi^2(2n-3)!!r}{2^{n-2}(n-1)!R^{2n-2}}\sum_{i=0}^{\infty}\frac{(n-\frac{1}{2})_i^2}{(i!)^2R^{2i}}\int_0^{2\pi}X^{2i}d\alpha. \tag{A-7}$$

The integrand in Eq. (A-7) can be expanded using binomial expansions to yield

$$J_n = \frac{\pi^2(2n-3)!!r}{2^{n-2}\,(n-1)!R^{2n-2}} \sum_{i=0}^{\infty} \frac{\left(n-\frac{1}{2}\right)_i^2}{i!R^{2i}} \sum_{j=0}^{i}\sum_{k=0}^{2j}\sum_{m=0}^{2i-2j} \frac{(j+1)_j(i-j+1)_{i-j}}{(2j-k)!k!(2i-2j-m)!m!}$$
$$\times r^{k+m}\epsilon^{2i-k-m}\sin^k\phi\cos^{2j-k}\psi\sin^{2i-2j-m}\psi\int_0^{2\pi}\sin^k\alpha\cos^m\alpha d\alpha, \qquad \text{(A-8)}$$

and the integral in Eq. (A-8) is evaluated as (eqn. (8.380(3)), page 908, [24])

$$\int_0^{2\pi}\sin^k\alpha\cos^m\alpha d\alpha = \begin{cases} 2B\left(\frac{k}{2}+\frac{1}{2},\frac{m}{2}+\frac{1}{2}\right) & k \text{ and } m \text{ are even integers,} \\ 0 & k \text{ or } m \text{ is an odd integer,} \end{cases}$$

and therefore the final form of $J_n$ becomes

$$J_n = \frac{\pi^2(2n-3)!!r}{2^{n-3}(n-1)!R^{2n-2}} \sum_{i=0}^{\infty}\sum_{j=0}^{i}\sum_{p=0}^{j}\sum_{q=0}^{i-j} \frac{\left(n-\frac{1}{2}\right)_i^2(j+1)_j(i-j+1)_{i-j}}{i!(2p)!(2q)!(2j-2p)!(2i-2j-2q)!R^{2i}}$$
$$\times r^{2p+2q}\epsilon^{2i-2p-2q}\sin^{2p}\phi\cos^{2j-2p}\psi\sin^{2i-2j-2q}\psi B\left(p+\frac{1}{2},q+\frac{1}{2}\right), \qquad \text{(A-9)}$$

where $p = k/2$ and $q = m/2$. We comment that although this seemingly lengthy expression appears complicated, it can be readily evaluated using standard algebraic computer packages such as Maple.

## References


1. T. Kar, J. Pattanayak, S. Scheiner, J. Phys. Chem. **105**, 10397 (2001)
2. A. Rochefort, Phys. Rev. B **67**, 115401 (2003)
3. N.W.S. Kam, T.C. Jessop, P.A. Wender, H. Dai, J. Am. Chem. Soc. **126**, 6850 (2004)
4. C.V. Nguyen, L. Delzeit, A.M. Cassell, J. Li, J. Han, M. Meyyappan, Nano Lett. **2**, 1079 (2002)
5. W. Wei, A. Sethuraman, C. Jin, N.A. Monteiro-Riviere, R.J. Narayan, J. Nanosci. Nanotechnol. **7**, 1 (2007)
6. T. Lin, V. Bajpai, L. Dai, Aust. J. Chem. **56**, 635 (2003)
7. C. Zhou, J. Kong, H. Dai, Appl. Phys. Lett. **76**, 1597 (2000)
8. C.L. Kane, E.J. Mele, Phys. Rev. Lett. **78**, 1932 (1997)
9. C. Kane, L. Balents, M.P.A. Fisher, Phys. Rev. Lett. **79**, 5086 (1997)
10. B.J. Cox, N. Thamwattana, J.M. Hill, J. Phys. A : Math. Theor **41**, 235209 (2008)
11. K. Schulte, J.C. Swarbrick, N.A. Smith, F. Bondino, E. Magnano, A.N. Khlobystov, Adv. Mater **19**, 3312 (2007)
12. P. Peumans, A.R. Forrest, Appl. Phys. Lett. **79**, 126 (2001)
13. N.A. Rakow, K.S. Suslick, Nat. **406**, 710 (2000)
14. L.Z. Zhang, P. Cheng, Phys. Chem. Comm. **6**, 62 (2003)
15. M.D. Ventra, S.T. Pantelides, N.D. Lang, Appl. Phys. Lett. **76**, 3448 (2000)
16. Y.C. Choi, W.Y. Kim, K.-S. Park, P. Tarakeshwar, K.S. Kim, J. Chem. Phys. **122**, 094706 (2005)

17. C.A. Hunter, K.R. Lawson, J. Perkins, C.J. Urch, J. Chem. Soc., Perkin Trans. **2**, 651 (2001)
18. S. Tsuzuki, K. Honda, T. Uchimaru, M. Mikami, K. Tanabe, J. Am. Chem. Soc. **124**(1), 104 (2002)
19. P. Hobza, J. Šponer, Chem. Rev. **99**, 3247 (1999)
20. T. Tran-Duc, N. Thamwattana, B.J. Cox, J.M. Hill, Math. Mech. Solids. **15**, 782 (2010)
21. L.A. Girifalco, M. Hodak, R.S. Lee, PNAS **62**, 13104 (2000)
22. S.D. Chakarova-Käck, E. Schröder, B.I. Lundqvist, D.C. Langreth, Phys. Rev. Lett. **96**, 146107 (2006)
23. R. Zacharia, H. Ulbricht, T. Hertel, Phys. Rev. B. **69**, 155406 (2004)
24. I.S. Gradshteyn, I.M. Ryzhik, *Table of Integrals, Series, and Products*, 7th edn. (Academic Press, Elsevier, USA, 2007)